

The Kauffman model on Small-World Topology

Carlos Handrey A. Ferraz and Hans J. Herrmann^{a,*}

^a*Departament of Physics, Universidade Federal do Ceara-UFC Campus do Pici,
PO Box 6030, CEP 60.455-760, Fortaleza, CE, Brazil*

Abstract

We apply Kauffman's automata on small-world networks to study the crossover between the short-range and the infinite-range case. We perform accurate calculations on square lattices to obtain both critical exponents and fractal dimensions. Particularly, we find an increase of the damage propagation and a decrease in the fractal dimensions when adding long-range connections.

Key words: Kauffman's automata, small-world topology, fractal dimension

PACS: 64.60.Cn, 64.60.Fr

1 Introduction

The Kauffman model [1] or more generally random Boolean networks have been studied in the past to describe genetic regulatory networks but are in fact very general because they do not assume any particular function of the nodes and can be applied on any topology. While in the late eighties much work has been done on the damage spreading transition renewed interest in this model has risen in the last years because of the issues of synchronisation[2], stability [3], control of chaos [4] and investigations on scale-free topologies[5,6]. A topology that is very characteristic for human networks is the small-world as introduced by Watts and Strogatz [7]. It is the purpose of this paper to present some numerical studies of the phase transition on the square lattice, complementing work by Stauffer [8], and then on its small-world variant showing the appearance of a new universality class.

* Corresponding Author.

Email addresses: `handrey@fisica.ufc.br` (Carlos Handrey A. Ferraz),
`hans@fisica.ufc.br` (Hans J. Herrmann).

Let us first review Kauffman cellular automata. The Kauffman model is a random mixture of all possible Boolean rules. Each of N lattice sites hosts a Boolean variable σ_i (spin up or down) which is either zero or unity. The time evolution of this model is determined by N functions f_i (rules) which are randomly chosen for each site independently, and by the choice of K input sites $\{j_K(i)\}$ for each site i . Thus the value σ_i at site i for time $t+1$ is given by:

$$\sigma_i(t+1) = f_i(\sigma_{j_1}(t), \dots, \sigma_{j_K}(t)) \quad (i = 1, 2, \dots, N) \quad (1)$$

Each Boolean function f_i is specified, once its value is given for each of the 2^K possible neighbour configurations. Here we are concerned with those cases where both the inputs and the chosen Boolean functions do not change with time (quenched model).

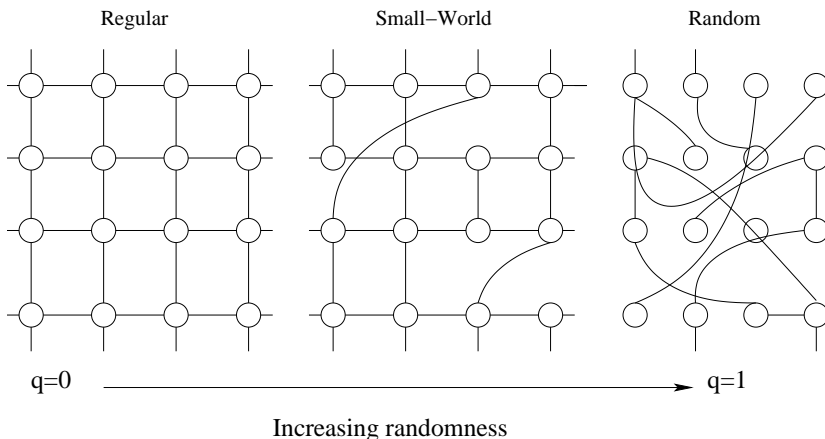


Fig. 1. Rewiring procedure

The Kauffman model has usually been considered in the last years, on one hand with an infinite range of interaction, known as the ‘mean-field’ approximation [9,10] in which for each site i , the K inputs are randomly chosen among the N spins. Such approximation was introduced to describe genetic interactions, to explain mutations and stability processes in biological genes. Indeed, this was the original proposal of the Kauffman model. On the other hand, this model has also been simulated on lattices with nearest-neighbour interactions, the so-called short-range case [8]. If one considers a square lattice, as we do here, for each site i the K inputs are just the four nearest neighbours, thus there being $2^4 = 16$ neighbor configurations, and therefore $2^{16} = 65536$ different possible rules. One can implement this by introducing a probability p of selecting a rule with the result spin up for each neighbor configuration and each lattice site. Of course, because of the symmetry of Boolean functions, one also has a probability $1-p$ that the result is spin down.

In the past, the connection topology had been assumed to be either completely random or completely regular. But many biological, technological and social networks lie somewhere between these two extremes. The ‘small-world’ topology seems to be very interesting for this purpose. In order to get more

knowledge about this intermediate range, we interpolate between regular and random networks by starting from a square lattice with N sites and $K=4$ inputs of nearest-neighbors and introducing a rewiring probability q to each input K connecting one site to any other, as indicated in Fig.1. Dynamical systems with small-world coupling exhibit enhanced signal-propagation speed and synchronizability. In particular, small damages, for example mutations on genetic material, spread more easily on small-world networks than on regular lattice.

In the present work, we have performed simulations based on a parallel bit manipulation technique called *multi-spin coding* [11] to attempt to determine the critical point p_c in analogy to percolation, both for the short-range case ($q = 0$) and for the small-world case ($q \neq 0$). To this end, we plot the normalized damage mass (see next section), i.e. our order parameter ψ , versus the parameter p . Once determined the critical points p_c for each case, we evaluate the critical exponents and the fractal dimensions.

2 ‘Damage Spreading’ on the Square Lattice

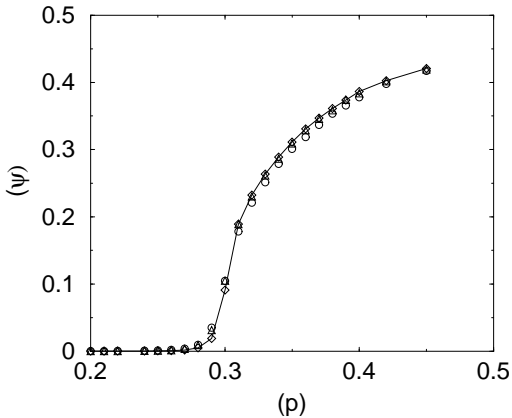


Fig. 2. Plot of ψ vs p for the short-range case ($q = 0.00$). Lattice sizes $L=256$; \circ , $L=384$; \triangle and $L=512$; \diamond .

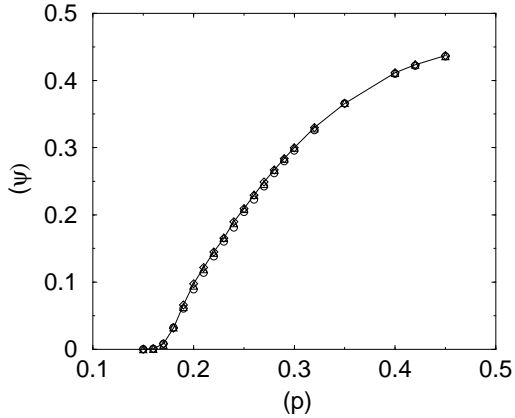


Fig. 3. Plot of ψ vs p for the small-world case ($q = 0.05$). Lattice sizes $L=256$; \circ , $L=384$; \triangle and $L=512$; \diamond .

With the objective of understanding how a single mutation spreads through genetic material, or how small hardware failures propagate on a computer architecture, we have compared two square lattices with identical sets of rules and almost identical Boolean variables at each site. The only difference between them consists in a small modification of few central Boolean variables (typically less than 1% of the number of sites). So one can observe the time-development of the two lattices and check the difference between them after a long time for each parameter value p . The difference between lattices is measured as the number of ‘spins’ that differ between the two lattices; this

difference is also known as Hamming distance $d(t)$ between the lattice configurations $\{\sigma_i(t)\}$ and $\{\rho_i(t)\}$:

$$d(t) = \frac{1}{N} \sum_i |\sigma_i(t) - \rho_i(t)|. \quad (2)$$

Following earlier works [8,12,13], we call this difference the ‘damage’. Further we define here the order parameter of the system as:

$$\psi = \lim_{d(0) \rightarrow 0} d(\infty), \quad (3)$$

and one can also define a susceptibility as:

$$\chi = \frac{\partial d(\infty)}{\partial d(0)}. \quad (4)$$

It has been observed that ψ as well as $1/\chi$ go to zero at some critical concentration p_c in systems of dimensions greater than one for the short-range case Kauffman model similar to the para-ferromagnetic phase transition. In other words, for all $p \leq p_c$, a small initial damage vanishes or remains small, i.e. belongs to a small cluster of ‘damaged spins’, after a sufficiently long time. One says that the system is in the frozen phase. On the other hand, for all $p > p_c$, a small initial damage spreads throughout a considerable part of the system. Then one says that the system is in the chaotic phase. Of particular interest is, however, the border case $p = p_c$ where fractal properties appear (see next section). To know more about phase transitions in Kauffman’s automata the reader should consult, for instance, Ref. [12]. As a way to find p_c in both

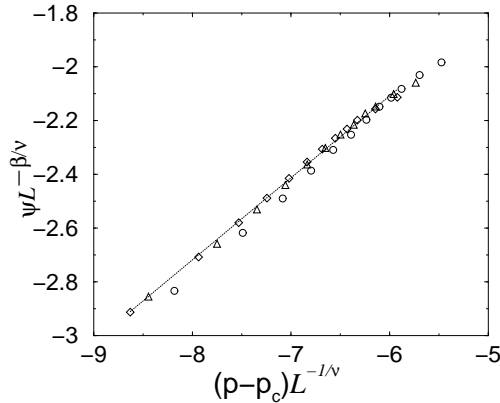


Fig. 4. Log-log plot of $\psi L^{-\beta/\nu}$ vs $(p - p_c) L^{-1/\nu}$ for the short-range case ($q = 0.00$). Lattice size $L=256$; \circ , $L=384$; \triangle and $L=512$; \diamond

the short-range and the small-world case, we plotted the order parameter ψ versus the parameter p for the case $q = 0$ (short-range) and $q = 0.05$ and 0.10 (small-world) for three different lattice sizes ($L=256$, 384 and 512) by flipping a small amount of regularly spaced central spins and taking an average over 100 runs for each point. Everything was calculated for up to 3×10^3 time-steps

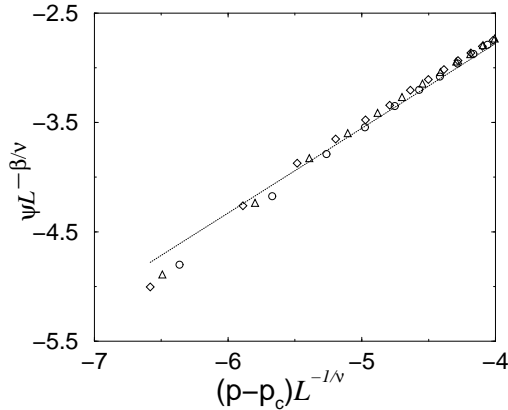


Fig. 5. Log-log plot of $\psi L^{-\beta/\nu}$ vs $(p - p_c)L^{-1/\nu}$ for the case ($q = 0.05$). Lattice size $L=256$; \circ , $L=384$; \triangle and $L=512$; \diamond

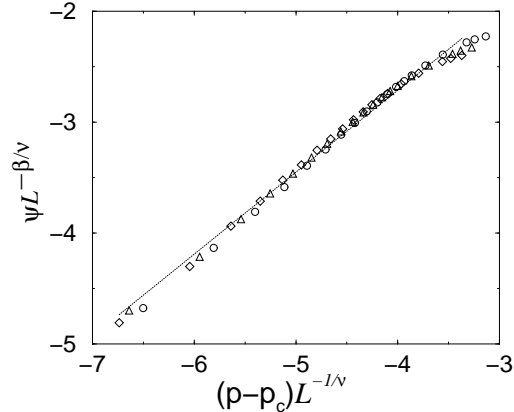


Fig. 6. Log-log plot of $\psi L^{-\beta/\nu}$ vs $(p - p_c)L^{-1/\nu}$ for the case ($q = 0.10$). Lattice size $L=256$; \circ , $L=384$; \triangle and $L=512$; \diamond

on an Intel Pentium IV processor. The updating speed using a *multi-spin coding* algorithm on an Intel machine which stores 64 spins in one computer word was about 2.44 updates per nanosecond for two configurations following the same iteration rules. Our results are shown in Figs. 2 and 3, respectively for $q = 0$ and $q = 0.05$. The transition between the frozen phase and the chaotic phase is seen to occur around $p_c = 0.30$ for the case $q = 0$ and around $p_c = 0.17$ and $p_c = 0.16$ for the cases $q = 0.05$ and $q = 0.10$, respectively.

Table 1

| | $q = 0.00$ | $q = 0.05$ | $q = 0.10$ |
|----------|-----------------|-----------------|-----------------|
| p_c | 0.30 | 0.17 | 0.16 |
| β | 0.31 ± 0.04 | 0.78 ± 0.04 | 0.74 ± 0.04 |
| γ | 2.50 ± 0.15 | 4.75 ± 0.20 | 4.65 ± 0.15 |

We estimate the critical exponents for each case by regarding the fraction of damaged sites (ψ) on each side of the critical point after a sufficiently long time. In the chaotic range ($p > p_c$), this fraction goes to zero as $(p - p_c)^\beta$. While in the frozen range, the ratio of the final damage to the small initial damage (χ) varies as $(p_c - p)^{-\gamma}$. We have made a collapse of all data in order to check the consistency of the obtained results by making use of the following scaling law:

$$\psi(L, p) = L^{-\beta/\nu} F((p - p_c)L^{-1/\nu}), \quad (5)$$

where L is the linear dimension of the lattice and ν is the exponent describing the divergence of the correlation length at p_c . Fig. 4 shows the data collapse for the case $q = 0$ at $p_c = 0.30$ which is in good agreement with Ref. [14], whereas the Figs. 5 and 6 show the data collapse for the case $q = 0.05$ and $q = 0.10$ at $p_c = 0.17$ and $p_c = 0.16$ respectively. Indeed, from Figs. 4, 5 and 6

we observe that the points following the scaling relation given by Eq. 5 have a slope of straight line equal to critical exponent β for each case. This could be an indication of the quality of our data. We have evaluated γ by means of the Eq. 4 at the transition threshold p_c . Our estimates together with the p_c values are shown in Table 1.

3 Fractal Dimensions

In analogy with percolation theory, we have determined the fractal dimensions d_{act} and d_t both for the short-range and the small-world cases by calculating the damage mass as well as the touching time on the lattice boundaries for several lattice sizes L at the critical point p_c .

The fractal dimension was defined by Stauffer [8] through the asymptotic proportionalities ($L \rightarrow \infty$) in the following way:

$$\langle M \rangle \sim L^{d_{act}} \quad (6)$$

$$\langle T_t \rangle \sim L^{d_t}, \quad (7)$$

where Eq. 6 says how the average damage increases with the lattice size L at the critical point, whereas Eq. 7 says how the average time for the damage spread increases with lattice size L at the critical point. The averages in Eqs. 6 and 7 are taken over those runs that eventually touch the upper or lower boundary of the square lattices. In this paper as in Ref. [15] we flipped a

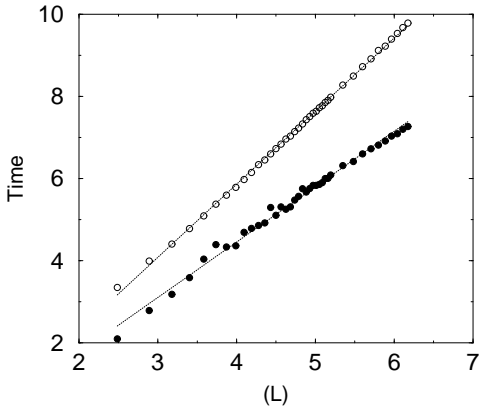


Fig. 7. Log-log plot of touching time vs L ; ●, damage vs L ; ○ for the short-range case ($q = 0.00$)

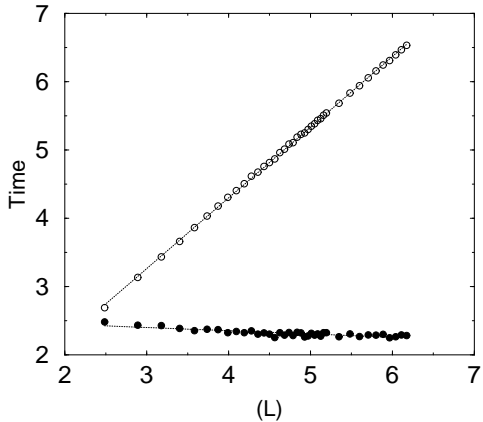


Fig. 8. Log-log plot of touching time vs L ; ●, damage vs L ; ○ for the small-world case ($q = 0.05$)

whole central line of spins at each time-step and let the system evolve until the final damage touches the lattice boundaries. Our results for the touching time T_t and the damage mass M at the touching time (averaged over 100 runs for

$q = 0$ and over 1000 runs for $q \neq 0$) are shown as a log-log plot of time vs L in Figs. 7 and 8, respectively for the short-range ($q = 0$) and the small-world ($q = 0.05$) case. Our numerical results for the short-range case ($q = 0$) turned out to be $d_{act} = 1.79$ and $d_t = 1.35$. These results are in good agreement with Ref. [14] and obey the scaling relations: From table 1, we have $\beta = 0.31$ and $\gamma = 2.48$. Assuming hyperscaling one has $d\nu = \gamma + 2\beta$, and we get $\nu = 1.55$. Standard percolation theory, suggests $d_{act} = d - \beta/\nu$, predicting $d_{act} = 1.80$. Our results for the small-world case ($q = 0.05$ and $q = 0.10$) were $d_{act} = 1.04$ and $d_t \approx 0$. Therefore one can see easily that at $q \neq 0$ the system no longer obeys the scaling relations of percolation.

4 Conclusion

With the use of our algorithm based on the *multi-spin coding* technique, we simulate Kauffman's automata, analyzing how small central damages spread on square lattices both in the short-range case and the small-world case. In this work, we have seen that for the small-world case the speed of damage spreading is larger than for short-range case. We numerically evaluate critical exponents β and γ for both cases. We also estimate the fractal dimension as being $d_{act} = 1.79$ for the short-range case and $d_{act} = 1.04$ for small-world case. Where for the latter case we can no longer observe scaling relations for percolation. Finally, we expect that these and other more elaborated calculations will be helpful to understand more general problems concerning the propagation of simple defects in complex systems.

5 Acknowledgement

We thank CAPES, CNPq, FUNCAP and the Max Planck prize for financial support.

References

- [1] Kauffman S. A., J. Theor. Biol. **22** (1969) 437.
- [2] Harvey I. and Bossomaier, T., proc. of the 4th Europ. Conf. on Artificial Life, (MIT Press, 1997) p.67.
- [3] Bilke S. and Sjunnesson F., Phys.Rev.E **65**, (2002) 016129.
- [4] Luque B. and Solé R. V., Europhys. Lett. **37** (1997) 597.

- [5] Aldana M., Physica D **185** (2003) 45.
- [6] Iguchi K., Kinashita S. and Yamada H., Phys. Rev. E **72**, (2005) 061901
- [7] Watt D. J. and Strogatz S. H., Nature **393** (1998) 440
- [8] Stauffer D., Phil. Mag. B **56** (1987) 901.
- [9] Derrida B., Phil. Mag. B **56** (1987) 917.
- [10] Drossel B., Mihaljev T. and Greil F., Phys. Rev. Lett. **94** (2005) 088701.
- [11] Friedberg R. and Cameron J. E. J. Chem. Phys. Rev. **52** (1970) 6049;
Hardy J., de Pazzis, O. and Pomeau Y., Phys. Rev. A **13** (1976) 1949;
Jacobs L. and Rebbi C., J. Comp. Phys. **41** (1981) 203;
Herrmann H. J., J. Stat. Phys. **45** (1986) 145.
Stauffer D., J. Phys. A **25** (1991) 909.
- [12] Derrida B. and Stauffer D., Europhys. Lett. **1** (1986) 739.
- [13] de Arcangelis L., J. Phys. A **20** (1987) L369.
- [14] Stauffer D., Physica D **38** (1989) 341.
- [15] Corsten M. and Poole P., J. Stat. Phys. **50** (1988) 463;
Coniglio A., de Arcangelis L., Herrmann H. J., Jan N., Europhys. Letts. **8** (1989)
315.